



**HAL**  
open science

# Wet creep of hardened hydraulic cements - Example of gypsum plaster and implication for hydrated Portland cement

Edgar Alejandro Pachon-Rodriguez, E. Guillon, G. Houvenaghel, Jean Colombani

## ► To cite this version:

Edgar Alejandro Pachon-Rodriguez, E. Guillon, G. Houvenaghel, Jean Colombani. Wet creep of hardened hydraulic cements - Example of gypsum plaster and implication for hydrated Portland cement. *Cement and Concrete Research*, 2014, 63, pp.67-74. 10.1016/j.cemconres.2014.05.004. hal-02309855

**HAL Id: hal-02309855**

**<https://univ-lyon1.hal.science/hal-02309855v1>**

Submitted on 17 May 2022

**HAL** is a multi-disciplinary open access archive for the deposit and dissemination of scientific research documents, whether they are published or not. The documents may come from teaching and research institutions in France or abroad, or from public or private research centers.

L'archive ouverte pluridisciplinaire **HAL**, est destinée au dépôt et à la diffusion de documents scientifiques de niveau recherche, publiés ou non, émanant des établissements d'enseignement et de recherche français ou étrangers, des laboratoires publics ou privés.

# Wet creep of hardened hydraulic cements - example of gypsum plaster and implication for hydrated Portland cement

Edgar Alejandro Pachon-Rodriguez<sup>a</sup>, Emmanuel Guillon<sup>b</sup>, Geert Houvenaghel<sup>b</sup>, Jean Colombani<sup>a,\*</sup>

<sup>a</sup>*Institut Lumière Matière; Université de Lyon; Université Claude Bernard Lyon 1; CNRS, UMR 5306; Domaine scientifique de la Doua, F-69622 Villeurbanne cedex, France*

<sup>b</sup>*Lafarge Centre de Recherche; 95, rue du Montmurier, BP 15, F-38291 Saint Quentin Fallavier cedex, France*

---

## Abstract

Gypsum plaster exhibits a dramatic creep when placed in a very humid environment. We have combined mechanical tests of wet bending creep of set plaster and holographic interferometry measurements of dissolution rate and diffusion coefficient to look for the origin of this wet creep. Both these experiments have been performed in absence and presence of various known anti-creep admixtures. It appears that the creep rate and dissolution rate are strongly correlated. This correlation has allowed to propose surface-driven pressure solution creep as mechanism of wet creep of gypsum plaster, i.e., the sequence dissolution in the grain boundary water/diffusion/precipitation at the grain surface. An order of magnitude analysis shows that this dissolution-diffusion-recrystallization series can also contribute to the creep of hydrated Portland cement.

---

\*Corresponding author, jean.colombani@univ-lyon1.fr

*Keywords:* A: Humidity, B: microstructure, C: creep, D: admixture, dissolution

---

## 1. Introduction

Hydraulic cements are mineral powders that harden under water, and subsequently remain cohesive in presence of water. They constitute the main materials of the building industry, used under the form of pastes to enable molding in the desired shape. Portland cement and gypsum plaster are the most used hydraulic binders because of their availability, low cost and easy installation. Hardened Portland cement and its derivatives (mortar, concrete) has also the virtue to be load-bearing, and hydrated plaster of Paris to be light, isolating and fire resistant. One of their limitations is their long-time plastic strain, or creep, mainly indoor for gypsum plaster and outdoor for hardened Portland cement. For gypsum, this creep is strongly enhanced by the presence of humidity.

Being chemically and structurally much simpler than hydrated cement pastes, this study is devoted to the creep of set plaster of Paris, with the aim to identify the underlying mechanisms and to estimate their applicability to the cementitious materials. Indeed the elimination, or at least limitation, of this drawback requires the understanding of its microscopic origin. Few studies have been devoted to the investigation of the link between the microstructure and the mechanical properties of set plaster. Concerning the influence of water, the few existing studies have brought some clues for the interpretation of the stiffness and resistance of set plaster in humid or wet environments. But up to now, the creep in presence of water had not re-

23 ceived any explanation. We have proposed recently that it derives from the  
24 dissolution of gypsum [1]. This finding has enabled to propose pressure so-  
25 lution creep as the mechanism of wet creep of set plaster. We detail here the  
26 experiments (mechanical tests and interferometric measurements) leading to  
27 this result and discuss its implications for hydrated Portland cement.

## 28 **2. Mechanical properties of gypsum plaster in presence of water**

29 Set plaster is constituted of intricate gypsum ( $\text{CaSO}_4, 2\text{H}_2\text{O}$ ) needles,  
30 roughly  $20\ \mu\text{m}$  long, obtained from the hydration of plaster of Paris ( $\text{CaSO}_4, \frac{1}{2}\text{H}_2\text{O}$ ).  
31 The cohesion of the material derives from the bonds between the needles and  
32 from the tenon and mortise joints between them [2]. It has been postulated  
33 about ten years ago that the bond between the needles is of the same nature  
34 as the bond between flocculated colloids [3]. Therefore the gypsum micro-  
35 crystallites should be linked via a nanometric water film. The attraction  
36 between them should stem from van der Waals interactions between the fac-  
37 ing charged faces and ionic correlations between the Debye layers developing  
38 in the water close to the surface, and the repulsion from the exclusion of  
39 the Debye layers. At the ends of the water layers, capillary forces develop  
40 at menisci and contribute to the cohesion between the needles. The balance  
41 between these forces determines the liquid film thickness. It has been added  
42 a few years later that the presence of “bridging”, i.e., solid, interfaces, be-  
43 side these “non-bridging” liquid interfaces between needles, is necessary to  
44 obtain a more comprehensive interpretation of the set plaster properties [4].  
45 This vision of the microstructure of the material enables to interpret several  
46 mechanical properties of wet or humid set plaster:

- 47 • it has been observed that Young’s modulus of set plaster decreases  
48 when the relative humidity increases [5, 6]. This can be interpreted by  
49 the fact that the equilibrium thickness of the water inter-needle layers  
50 increases with the relative humidity enhancement, from  $\sim 1$  nm in dry  
51 conditions to  $\sim 10$  nm in humid ones [3]. And a thicker layer induces  
52 a weaker bond between needles. The assumption has been made that  
53 this weakened connection can result in a reversible slip between some  
54 microcrystallites, increasing the elastic strain, thus decreasing Young’s  
55 modulus. The bridging bonds deform only by elastic bending and guar-  
56 antee that no irreversible strain occurs.
- 57 • The flexural strength, i.e., the bending failure stress of this brittle ma-  
58 terial, has also been seen as decreasing when the material is soaked in  
59 water [7] or when it adsorbs water [8]. This feature can also be ascribed  
60 to the thickening of the water layers in a humid environment. Indeed  
61 the resulting slip between microcrystallites implies a lower contribution  
62 of the non-bridging bonds to the strength, so a lowered failure stress.
- 63 • It has also been observed that, if the hardness of a set plaster sample  
64 decreases after being plunged in water, the hardness recovers its initial  
65 value once the sample is dried [7]. The reversibility of the influence  
66 of water can again be interpreted by the fact that the mechanical  
67 resistance of the material reflects the values of the inter-needle water  
68 slab thickness, in equilibrium with the quantity of water available. If  
69 more water is available, the layer thickens and the cohesion diminishes,  
70 and vice-versa.

### 71 **3. Wet creep of gypsum plaster**

72 Beside these successes of the theory, one should mention that unfortu-  
73 nately it does not provide any mean to understand the increase of creep in  
74 a humid environment [9, 10]. Indeed creep is a slow process occurring over  
75 periods of days or months, whereas the equilibration of the intercrystalline  
76 water layers is a quasi-instantaneous mechanism. Thereby the progressive  
77 plastic strain occurring during creep cannot be explained by a progressive  
78 increase of the slab dimension leading to a loss of cohesion.

79 We show here that the wet creep of set plaster is a consequence of a  
80 phenomenon called pressure solution creep (figure 1). When an external  
81 stress, or simply its own weight, is applied to a gypsum board, the gypsum  
82 needles are subject to local stresses. These stresses induce an increase of the  
83 chemical potential of the gypsum. So when water is present, in particular in  
84 the intercrystalline contacts, to recover chemical equilibrium, the chemical  
85 potential of the liquid increases also to equalize with the one of the solid. This  
86 leads to the enhancement of the solubility of gypsum, thereby to a dissolution  
87 of the solid in the liquid. Therefore concentration gradients appear along the  
88 water layers, which induce Fick diffusion of dissolved gypsum. When the  
89 sulfate and calcium ions reach areas without stress, their solubility recovers  
90 its initial value and they precipitate on the solid at rest. This dissolution-  
91 diffusion-precipitation series continues as long as the local stress exists, and  
92 induces a transfer of matter from high stress to low stress regions. By this  
93 way a plastic strain occurs, which accommodates the applied stress, and the  
94 material creeps.

95 This phenomenon is well known in geology. It has been ascribed several

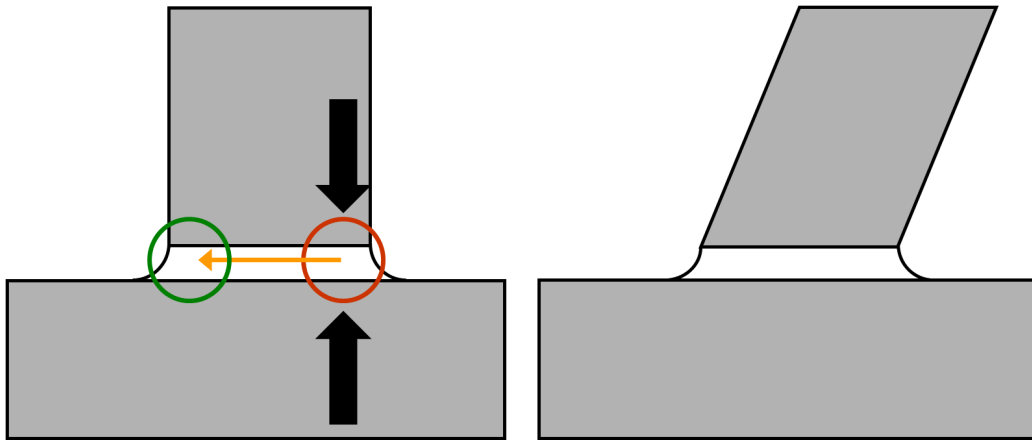


Figure 1: Sketch of the consecutive steps of pressure solution creep in gypsum plaster: an external load creates a local compression stress between two gypsum needles, which induces dissolution, diffusion of the dissolved species, and recrystallisation in a non-stressed area. This sequence induces a local transfer of matter, so a macroscopic plastic strain.

96 contributions to the upper crust evolution, for instance during non-seismic  
 97 strain of active faults, or for the transformation of loose sediments into co-  
 98 hesive sedimentary rocks [11]. Pressure solution creep has in particular be  
 99 evidenced in wet gypsum particulates under uniaxial and hydrostatical load  
 100 [12, 13].

101 Numerous experiments of pressure solution creep in water have been per-  
 102 formed in laboratory, with the final aim of understanding geological situa-  
 103 tions. Many of these studies use model systems or model configurations from  
 104 which we can learn on the basic mechanisms and characteristic kinetics of  
 105 pressure solution [11]. But their specific features, generally devoted to geol-  
 106 ogy, make their application to industrial materials difficult. For instance, the  
 107 available works on pressure solution in gypsum study low porosity assemblies

108 of non-cohesive quasi-spherical gypsum crystallites,. All of these character-  
109 istics differ from industrial gypsum, thereby making the application of these  
110 studies difficult to building materials. We have not found such a study in the  
111 materials science field. Therefore a protocol enabling to validate the existence  
112 of pressure solution in the creep of humid gypsum plaster is necessary.

113 Before going on, we would like to recall that it was formerly thought that  
114 the decrease of the mechanical strength of set plaster with moisture could  
115 be due to the dissolution of small gypsum crystals, precipitated at the end  
116 of the plaster setting and bridging the gypsum needles [14, 15]. This phe-  
117 nomenon was sometimes misleadingly called "dissolution-recrystallization".  
118 Pressure solution creep mentioned here also involves dissolution and recryst-  
119 tallization but in a totally different way: dissolution occurs at high stress  
120 regions of inter-needle contacts and recrystallization at low stress regions or  
121 at the needles surface. No microcrystal appears or disappears. This hypoth-  
122 esis of dissolving-recrystallizing microcrystals was unambiguously discarded  
123 by hardness and bending tests in various conditions of plaster setting and  
124 relative humidity [7].

125 To establish a protocol of validation of the presence of pressure solution  
126 creep, we benefit from the methodology of the works performed on the ge-  
127 ological side. In these studies, the presence of pressure solution creep, and  
128 its exact nature, is usually determined by measuring the creep kinetics. The  
129 slowest step in the reaction-transport-recrystallization sequence limits the  
130 matter transfer rate, so drives the whole kinetics and determines the evolu-  
131 tion laws.

132 The theoretical determination of the exact expression of  $\varepsilon(t)$ , the strain



133 evolution with time, requires to define precisely many parameters: order of  
134 the chemical reaction, reactive surface area, thickness of the liquid slab, locus  
135 of the precipitation sites, porosity, size distribution of the mineral grains,  
136 width of the solid contacts, . . . The final  $\varepsilon(t)$  curves have been found to be  
137 highly dependent on the above characteristics of the system and on their  
138 interplay. A particularly complete modelization of pressure solution creep in  
139 sandstone for instance can be found in Ref. [16].

140 As no complete pressure solution modelization of a highly porous medium  
141 like set plaster exists, we have to make with first-order models, bringing at  
142 least trends of the strain evolution with time. We have chosen the acclaimed  
143 model of Raj [17]. His modelization considers the creep of a unique stressed  
144 cubic mineral sample in a solvent present in channels at its surface. It states  
145 that :

- 146 • if the kinetics is driven by the mass transport (due in general to a low  
147 flow rate of diffusion in tiny channels), the strain rate writes:

$$d\varepsilon/dt \sim \sigma D s/d^3 \quad (1)$$

- 148 • if the kinetics is driven by the surface reaction (due to its slowness),  
149 the strain rate writes:

$$d\varepsilon/dt \sim \sigma k s/d \quad (2)$$

150 In these expressions,  $\sigma$  is the applied stress,  $D$  the diffusion coefficient of the  
151 dissolved species,  $k$  the **reaction** rate constant of the mineral,  $s$  its solubility  
152 and  $d$  the characteristic size of the constrained interface.

153 In geological laboratory experiments, the limiting step is estimated in  
154 varying the grain size  $d$  and determining if the strain rate scales as  $d^{-1}$

155 or  $d^{-3}$ . In our case, varying the gypsum crystallites size in set plaster is  
156 difficult. To identify the limiting stage, we have benefited from the existence  
157 of admixtures added to the plaster industrially to limit the humid creep.  
158 These additives are efficient in slowing down the creep strain rate, but again,  
159 their mechanism of action is not understood yet. So the idea of our work is to  
160 find which factor of the above expressions, if any, these admixtures modify,  
161 to lower the strain rate, thus indicating the working mechanism of creep.

## 162 4. Experiments

163 In equations 1 and 2, the parameters the knowledge of which is needed  
164 are  $d$ ,  $s$ ,  $k$ ,  $D$  and  $d\varepsilon/dt$ .

### 165 4.1. Admixtures

166 The investigated anti-creep admixtures are a tartaric acid ( $C_4H_6O_6$ ) / boric  
167 acid ( $H_3BO_3$ ) mixture, Trilon P, i.e., a commercial version of a sodium salt of  
168 a polyamino carboxylic acid ( $C_{10}H_{16}N_2O_8$ , CAS no. 454473-50-8), Sequion  
169 50K33 and Dequest 2054, i.e., two commercial versions of the hexamethylene-  
170 diamine tetra(methylene phosphonic acid) hexapotassium salt ( $C_{10}H_{22}K_6N_2O_{12}P_4$ ,  
171 CAS no. 38820-59-6), and STMP, i.e., sodium trimetaphosphate ( $Na_3P_3O_9$ ).  
172 The acid mixture is made of 1/6 of tartaric acid and 5/6 of boric acid in  
173 weight.

### 174 4.2. Bend creep tests

175 For the bend tests, gypsum (from Mazan quarry, France) is ground and  
176 dehydrated to make plaster ( $CaSO_4, \frac{1}{2}H_2O$ ). The resultant powder is mixed  
177 with water to make a paste with a water/plaster weight ratio of 0.8, bringing

178 a convenient compromise between the fluidity of the paste and the porosity  
179 of the final product (57%). The mixture is cast in a parallelepipedic mold,  
180 placed in a closed vessel during 24 h to achieve complete hydration, dried, and  
181 stored in calcium sulfate saturated water until the test, to avoid dehydration  
182 [15]. The same protocol was also followed with water containing the various  
183 admixtures.

184 Standard bend tests have been performed to measure the creep strain rate  
185 of set plaster. The above-described samples were loaded in the middle on  
186 the top face and supported at their ends. The deflection was recorded with a  
187 Linear Variable Differential Transformer displacement sensor every 2 h during  
188 15 days. During the tests, the beams were immersed in water —to study  
189 wet behavior— saturated with calcium sulfate —to avoid normal dissolution  
190 and be sure to observe, if any, pressure dissolution. The maximum load  
191 was chosen as 20% of the tensile strength, measured for each batch on one  
192 sample before the test, to remain outside the stress range where subcritical  
193 crack growth inside the samples is expected, risking to blur the results [9, 18].

194 The force and displacement are converted in the stress  $\sigma$  and strain  $\varepsilon$  at  
195 the top face in the middle of the beam with the elastic approximation:

$$\sigma = \frac{3PL}{2wh^2} \quad \text{and} \quad \varepsilon = \frac{6h\delta}{L^2} \quad (3)$$

196 In these expressions,  $P$  is the load,  $L$  the support span,  $w = 20$  mm the  
197 width of the beam and  $h = 20$  mm its height.

198 The zero-stress curve inside the beam may depart from the center of the  
199 beam, due to non-symmetry of the compressive and tensile strain mechanism,  
200 which may make these formulas non valid. But the determination of the exact  
201 stress field is not possible and would deserve a study for itself.

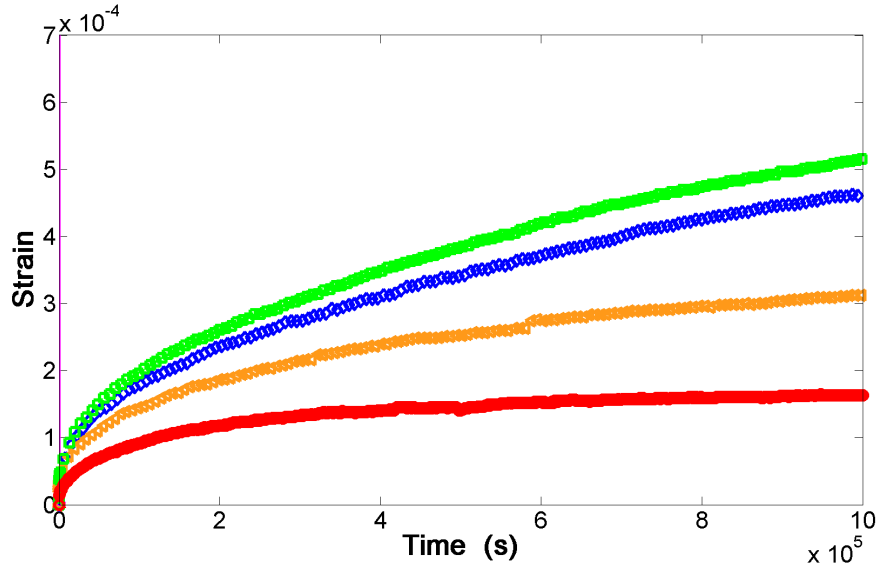


Figure 2: Evolution with time of the bending strain for the gypsum plaster samples manufactured with 0.15% Sequion in the preparation water. The applied stress, from the bottom to the top curve is 0.244 (red), 0.332 (orange), 0.356 (blue) and 0.386 (green) MPa.

202 An example of  $\varepsilon(t)$  curves at various stresses for one admixture is shown in  
 203 figure 2. The strain rate  $d\varepsilon(t)/dt$ , needed for the test of the above-mentioned  
 204 equations is obtained in derivating the experimental  $\varepsilon(t)$  curves numerically.  
 205 From it, the creep compliance rate  $(d\varepsilon(t)/dt)/\sigma$  is computed. All strain-time  
 206 data and curves for all admixtures and stresses can be found as Supplemen-  
 207 tary Material.

208 A parameter that may play a role in the elaboration of the samples is  
 209 the concentration of admixture in the water used to manufacture the gyp-  
 210 sum from the plaster powder. Several concentrations between 0.05% and  
 211 0.5% in weight have been tested for each additive. The creep results have  
 212 been found to be independent on the concentration, except for the smallest

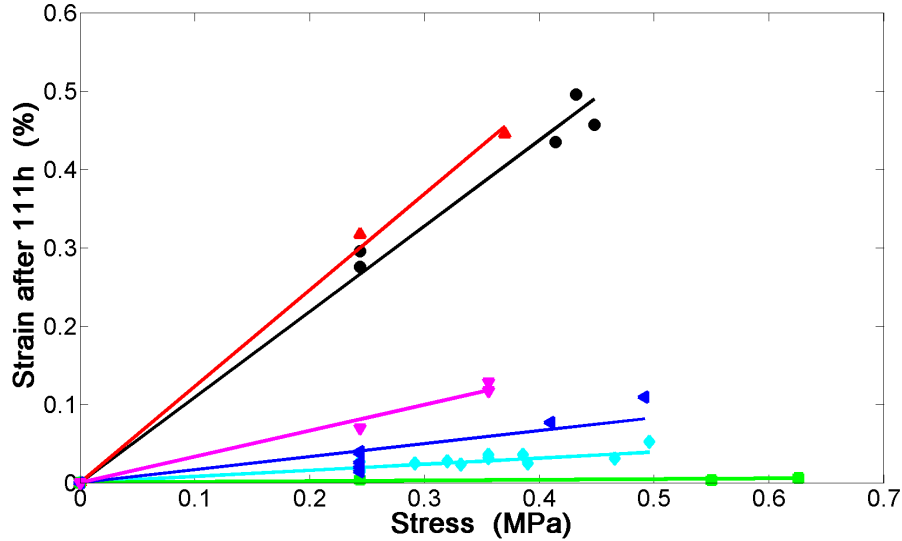


Figure 3: Bend strain  $\varepsilon$  after 111 h versus applied stress  $\sigma$  for the various admixtures: pure water (black circles), boric/tartaric acid (red upward triangles), Trilon (pink downward triangles), Dequest (blue leftward triangles), Sequion (light blue diamonds), STMP (green squares).

213 concentrations ( $\lesssim 0.1\%$ ) where the anti-creep action is less efficient.

214 The strain obviously depends on the bending stress. To get an estimate  
 215 of the evolution of the creep intensity with the applied stress, the value of the  
 216 bend strain at one given time (namely 111h) has been drawn versus the bend  
 217 stress in figure 3. It can be stated that the creep is roughly proportional to  
 218 the applied stress in the range investigated in this study.

#### 219 4.3. Contact size

220 The determination of the inter-needle contact size  $d$  is not a trivial task  
 221 and for this we have performed scanning electron microscopy observations of  
 222 the microstructure of the set plaster samples (figure 4). For all the admix-

223 tures used, the microstructure remains of the acicular type. None of them  
224 reveal lenticular or columnar habit, sometimes encountered in natural gyp-  
225 sum, depending on the impurities adsorbing on specific crystalline planes.  
226 The characteristic size of the microcrystals is similar at first order in all pic-  
227 tures and we have considered that the contact size  $d$  should also be similar  
228 among all samples. For the computations in next section, the average value  
229 of  $d = 1 \mu\text{m}$  has been chosen.

230 Nevertheless we can mention that gypsum plaster elaborated with Se-  
231 quion reveals unexplained micrometer-size etch pits at the needles surface.  
232 Whereas we have seen that, according to the SEM pictures, the influence  
233 of the additives on the set plaster microstructure is not significant, we have  
234 attempted to get a further evidence of this lack of influence in testing another  
235 protocol of elaboration of the samples. In this process, all solid samples are  
236 first elaborated from plaster and pure water, in the absence of any admix-  
237 ture. Subsequently, each sample is soaked during 12h in water containing  
238 a given concentration of additive, to make the molecules impregnate the  
239 gypsum crystallites network of the material. The creep bend tests are then  
240 performed as detailed in section 4.2. The interest of this procedure is to  
241 guarantee that all samples have strictly the same microstructure, having all  
242 been elaborated in pure water.

243 Figure 5 shows the creep curves for one admixture present in the impreg-  
244 nation water at various concentrations. As the applied stresses are almost  
245 similar, the difference between the various curves can be ascribed to the con-  
246 centration of additive in the soaking water. The more concentrated in addi-  
247 tive the impregnation solution, the more efficient the anti-creep effect. The

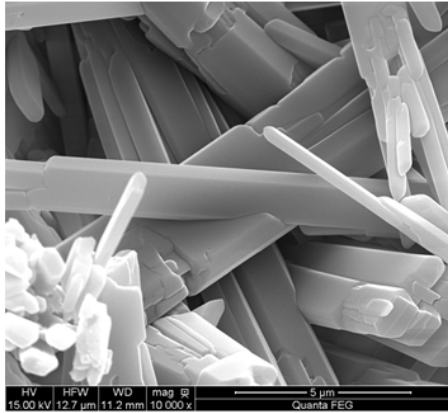
248 origin of this evolution is to be searched in the variation of the dynamics of  
249 adsorption and diffusion in a porous medium of the admixture for the various  
250 concentrations. This result seems to indicate that the quantity of molecules  
251 inside the sample is not the same for the various concentrations, even with  
252 the long impregnation time we have chosen. The adsorption and diffusion  
253 dynamics may be different from one admixture to another, which makes the  
254 comparison between the results obtained with the various additives quite del-  
255 icate. Therefore, we have abandoned this process and exclusively used the  
256 protocol presented in the previous section, where we have the certainty that  
257 the molecules are embedded in the samples.

#### 258 *4.4. Solubility*

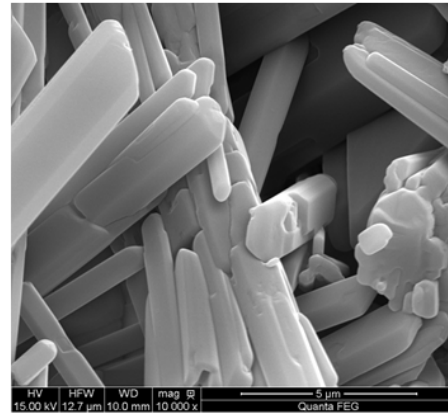
259 The solubility of gypsum in aqueous solutions of the various admix-  
260 tures has been determined by induced coupled plasma atomic emission spec-  
261 troscopy. Certainly due to the low concentration of additive here, no depart-  
262 ure from the solubility of gypsum in pure water (2 g/L, 15 mmol/L) has  
263 been found, whatever the added product.

#### 264 *4.5. Dissolution rate constant*

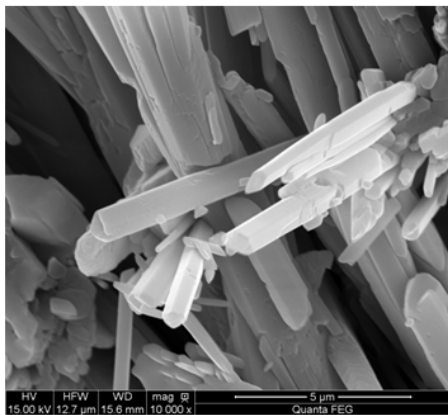
265 The gypsum-water interfacial reaction rate constant is also needed, being  
266 either the dissolution or precipitation rate constant in Raj's equation. De  
267 Meer and Spiers identified precipitation as the driving mechanism, which  
268 can be expected in their low porosity system, where unstressed precipitation  
269 sites are rare [13]. But the dissolution and precipitation rate constants should  
270 be close. Indeed the rate of attachment and detachment of ions at a solid  
271 surface are strongly linked, and a change of the surface reactivity influence



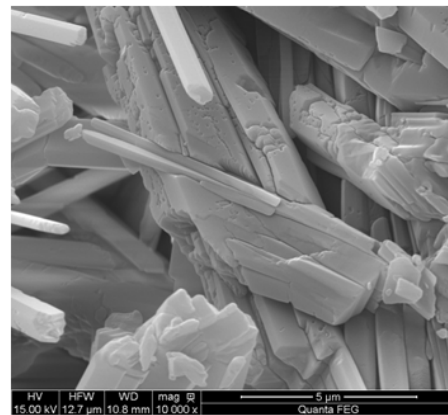
water



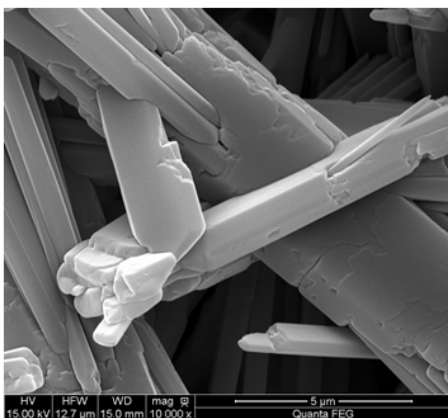
tartaric/boric acid



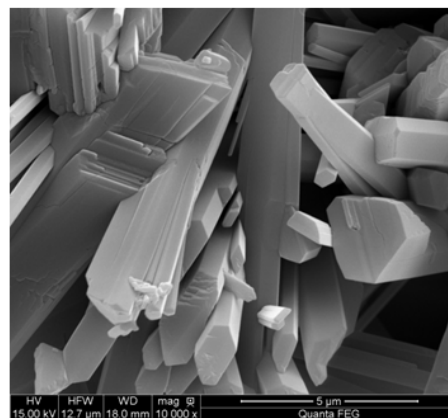
Trilon



Sequion



Dequest



STMP

Figure 4: Scanning electron microscope pictures of set plaster samples, pure and elaborated with the various admixtures. The dimension of the images is  $12.7 \times 11.0 \mu\text{m}^2$ .



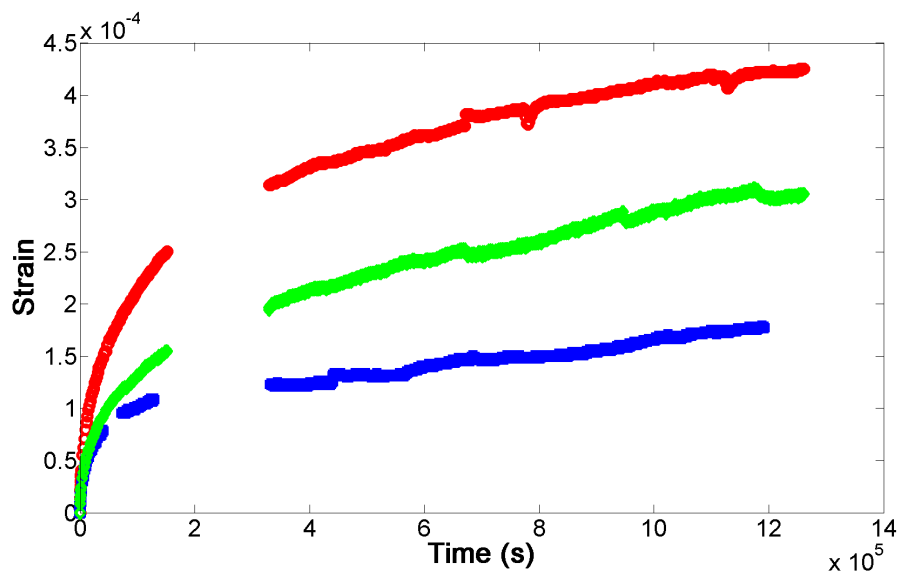


Figure 5: Evolution with time of the bending strain for the pure gypsum plaster samples impregnated by Sequion. From the top to the bottom curve, the concentration of Sequion in the impregnation water is 0.50 g/L for a 0.406 MPa stress (red), 4.97 g/L for a 0.524 MPa stress (green) and 9.94 g/L for a 0.496 MPa (blue).

272 both [19]. We have chosen to study the dissolution rate constant. But if  
273 a correlation between creep and dissolution is found and shows that the  
274 phenomenon is interface-driven, it is very likely that a correlation between  
275 creep and precipitation also exists.

276 The measurement of the dissolution rate constant is a delicate task. As  
277 we have shown in preceding studies, the usual solution chemistry methods  
278 provide dissolution rates blurred by mass transport phenomena (diffusion,  
279 convection) [20, 21]. As the possible effect of admixture on the dissolution  
280 rate constant may be tiny, the standard dissolution measurement techniques  
281 were not appropriate and we have used an alternative methodology, holo-  
282 graphic interferometry. This technique has been described in detail in Ref.  
283 [22]. It presents two major advantages. First the experiment is performed in  
284 quiescent water, thereby avoiding any convective disturbance. Secondly the  
285 concentration is directly measured at the solid-liquid interface, whereas in  
286 standard methods it is measured in the flowing liquid far from the surface.

287 The dissolution rate constant  $k$  of gypsum of the same origin as in the  
288 bend tests —to allow comparison— in water containing the various admix-  
289 tures has been measured by holographic interferometry and for all of them,  
290  $k$  has been found to be modified by the admixture [23]. The results are  
291 summarized in table 1.

#### 292 *4.6. Diffusion coefficient*

293 The holographic interferometry experiments have also the advantage to  
294 give access to the diffusion coefficient  $D$  of dissolved gypsum in water. There-  
295 fore  $D$  has been measured for gypsum in water containing the various ad-  
296 mixtures and it has been seen that this coefficient is almost constant for all

Admixture	$k$ ( $10^{-6}$ mol m $^{-2}$ s $^{-1}$ )	$D$ ( $10^{-10}$ m $^2$ s $^{-1}$ )
Without	46	7.1
Tartaric-boric acid	74	5.9
Trilon	21	4.3
Sequion	11	6.1
Dequest	8.0	4.9
STMP	3.3	6.5

Table 1: Dissolution rate constant  $k$  and diffusion coefficient  $D$  of gypsum in water containing various admixtures, measured by holographic interferometry.

297 admixtures, probably due to the low concentration of the products, as shown  
298 in table 1.

## 299 5. Results and discussion

300 Before testing our assumption of pressure solution creep using all the  
301 experiments described in the preceding section, we would like to focus first  
302 on the  $\varepsilon(t)$  curves. They constitute the first systematic study of the wet  
303 creep of gypsum plaster. By fitting the curves, we have noticed that all of  
304 them obey to a power law:  $\varepsilon(t) = At^n$ , with  $n < 1$ . Thereby, we see that  
305 a consolidating mechanism is active during the wet creep, which slows down  
306 progressively the strain. The creep exponent  $n$  depends on the admixture  
307 with which the set plaster sample has been manufactured: 0.69 for pure  
308 water, 0.71 for boric/tartaric acid, 0.52 for Trilon, 0.34 for Sequion, 0.39 for  
309 Dequest and 0.38 for STMP. It is striking to state that it evolves from  $\sim 2/3$   
310 to  $\sim 1/3$  from pure water to the most efficient anti-creep admixture. Figure  
311 6 illustrates this evolution. We have not found yet the origin of this ability

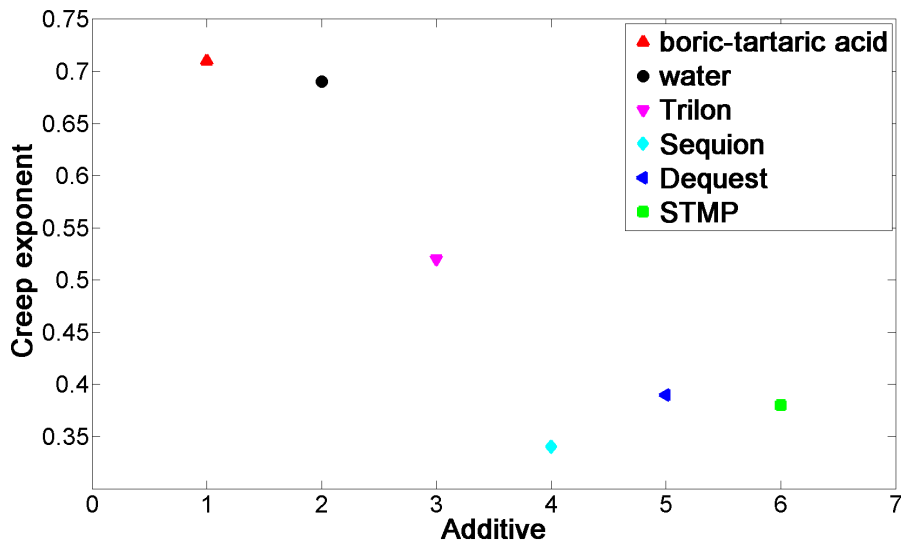


Figure 6: Bend creep exponent of wet gypsum plaster manufactured with the various admixtures.

312 of admixtures to lower the creep exponent. We can just mention that the  
 313  $1/3$  exponent in presence of anti-creep products recalls both i) the exponent  
 314 of Andrade creep, i.e., diffusive creep in non-porous materials, and ii) the  
 315 pressure solution creep exponent observed in NaCl single crystals by Dysthe  
 316 et al. [24].

317 We are now able to test the agreement between our experiments and  
 318 equations 1 and 2. For the first one, we have plotted in figure 7 the creep  
 319 compliance rate  $\dot{\varepsilon}(t_0)/\sigma$  as a function of  $D s/d^3$ . **To gain statistical accuracy,**  
 320 **each dot in this figure represents an average of the results of a few experiments**  
 321 **performed at quasi-equal stresses.** The question of the choice of  $t_0$  arises.  
 322 Indeed the  $\varepsilon(t)$  curves are non linear. We have chosen  $t_0 = 1 \times 10^5$  s, in  
 323 the middle of the investigated time, but we have checked otherwise that the

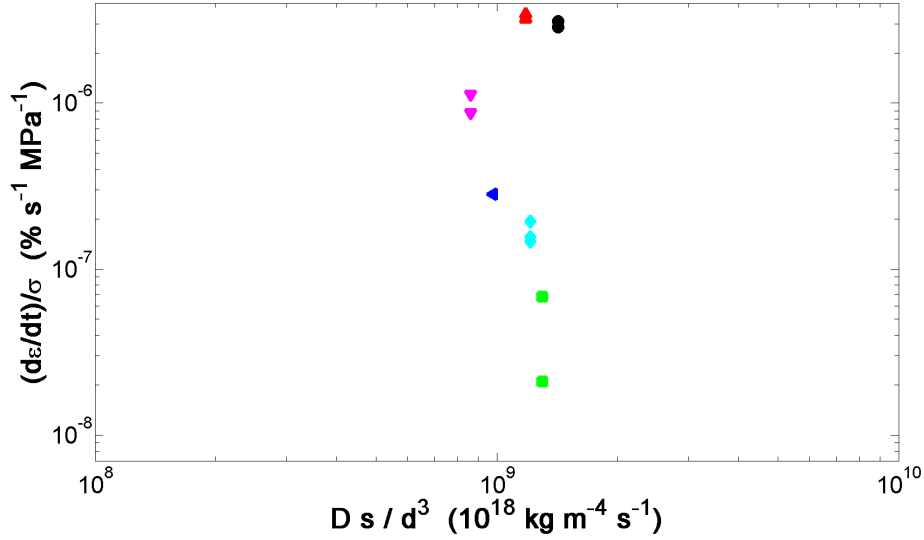


Figure 7: Compliance rate for wet bending creep of gypsum plaster elaborated with a given additive at  $t_0 = 1 \times 10^5$  s, as a function of a coefficient proportional to the diffusion coefficient of dissolved gypsum in a solution of the same additive. Red upward-pointing triangles: tartaric/boric acid; black circles: pure water; pink downward-pointing triangles: Trilon; blue left-pointing triangles: Sequin; light blue diamonds: Dequest; green squares: STMP.

324 obtained correlation is valid all along the experiments. As can be seen in  
 325 figure 7, no correlation is observable between the 2 factors. The compliance  
 326 rate varies of 2 orders of magnitude among the admixtures, whereas the  
 327 diffusion coefficient remains almost constant ( $s$  and  $d$  keeping always the  
 328 same value). Therefore the diffusion velocity of the gypsum dissolved species  
 329 has no influence on the creep kinetics, which discards the diffusion-driven  
 330 pressure solution creep as creep mechanism.

331 Now, to test equation 2, we have drawn in figure 8 the creep compliance  
 332 rate  $\dot{\epsilon}(t_0)/\sigma$  as a function of  $k s/d$ . Again, each dot in the figure stands for an

333 average of the results of a few experiments performed at close stresses. Here  
334 we see a very strong correlation between the two quantities. Indeed  $\dot{\epsilon}(t_0)$   
335 and  $k$  evolve of almost 2 orders of magnitude from pure water to the most  
336 efficient anti-creep coefficient, giving rise to the observed coupling between  
337 the two parameters in figure 8. This correlation is a strong support to the fact  
338 that the wet creep of gypsum plaster is a reaction-driven pressure solution  
339 creep. Again the correlation is shown at  $t_0 = 1 \times 10^5$  s in figure 8 but we  
340 have checked that the correlation exists all along the experiments. If the  
341 link between dissolution velocity and creep velocity is established, we have  
342 to mention that the first order model of the phenomenon we have used (in  
343 absence of a more complete model) does not catch the exact correlation. The  
344 model predicts  $\dot{\epsilon} \sim (\sigma ks/d)^m$  with  $m = 1$  and we find  $m = 1.3$  to  $1.7$ , slightly  
345 evolving between the beginning and the end of the experiment.

346 We would like to mention here the compressive creep tests performed by  
347 Hoxha et al. with natural gypsum rocks [25]. They mention that the duration  
348 of their experiments is too short ( $\sim 15$  days) to evidence pressure solution.  
349 Therefore they explain the expansion of their samples by a mechanism of  
350 reversible migration of water molecules, from the solid to the pore space. As  
351 shown here, the consequence of pressure solution creep may be observable  
352 even for such short period of time. **With the material at hand, we are not able  
353 to explain why they do not observe precipitation-limited pressure solution  
354 creep like de Meer & Spiers with a system of similar porosity [13].**

355 Now that the basic mechanism of the wet creep of gypsum plaster is  
356 elucidated, a detailed theoretical analysis of pressure solution in an as porous  
357 material as gypsum plaster would enable to make quantitative predictions

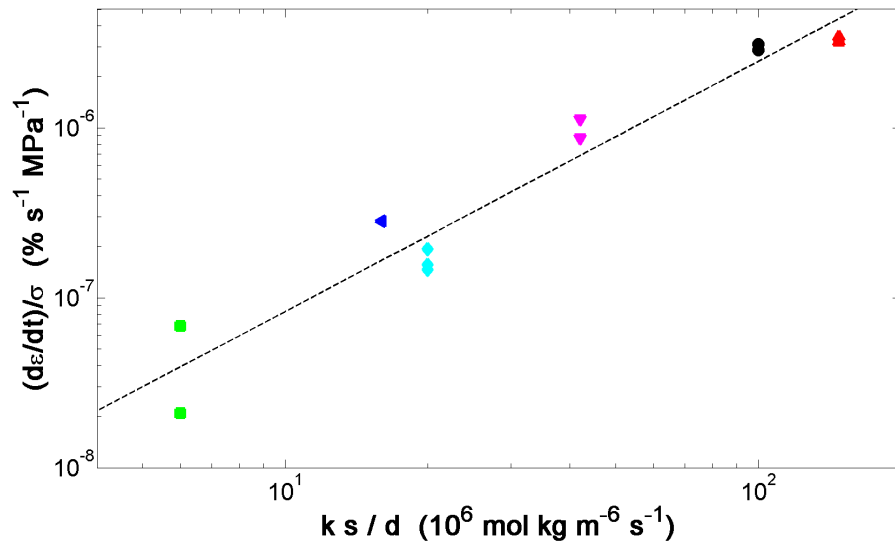


Figure 8: Compliance rate for wet bending creep of gypsum plaster elaborated with a given additive at  $t_0 = 1 \times 10^5$  s, as a function of a coefficient proportional to the dissolution rate constant of gypsum in a solution of the same additive. The color code is the same as in figure 7. The black dashed line is a linear fit of the data.

358 about its kinetics. But knowing that the dissolution kinetics is at the basis  
359 of wet creep enables to try to find tools against this drawback of the material.

## 360 **6. Implications for hydrated Portland cement**

361 Despite being the manufactured material most used on earth, the struc-  
362 ture and cohesion of hydrated Portland cement is not perfectly understood  
363 yet. Along a schematic view, a hydrated Portland cement paste can be con-  
364 sidered as a flocculated colloidal suspension of calcium-silicate-hydrate (C-S-  
365 H), i.e.,  $(\text{CaO})_{1.7}(\text{SiO}_2)(\text{H}_2\text{O})_{1.8}$  [26], nanometric particles, called gel, with  
366 partial crystallinity [27].  $\text{Ca}(\text{OH})_2$  nanocrystallites, and other minor hydra-  
367 tion products, are also present in the gel. Like in standard colloidal gels, the  
368 remarkable strength of this hydraulic cement stems from electrostatic and  
369 ionic correlation forces between the particles via the water layers between  
370 them [28]. Capillary forces contribute also in unsaturated materials, where  
371 water-air menisci are present.

372 It is generally admitted that C-S-H is found in hydrated pastes in 2 or  
373 3 forms, of identical chemical composition, but clearly distinct organizations  
374 and densities [3, 29, 30]. The proportion of these phases varies with the  
375 water/cement ratio used to manufacture the cement paste, the drying, and  
376 the aging of the material. This structural heterogeneity induces a multi-scale  
377 porosity, also evolving with the just-mentioned parameters.

378 One major concern about cementitious materials is their aging, in the  
379 form of shrinkage, creep, fractures, ... partly due to the slow drying of the  
380 products of cement hydration [31]. It has been shown that the concrete creep  
381 strain results exclusively from the irreversible strain of the cement hydration



382 products [32] and the creep of hardened cement is still an active field of  
383 research [30].

384 We discuss here only about wet creep, i.e., the plastic strain under small  
385 load of the water saturated material. In these conditions, capillary menisci  
386 inside the material are absent, which suppresses a major source of aging of  
387 the material. Therefore in this case the creep cannot derive from shrinkage  
388 induced by water loss, and corresponding models do not apply [31]. Recent  
389 assumptions of creep origin applying in this situation are: reorganization  
390 of high density phase globules, analog to dislocation migration in crystals  
391 [29], reorganization of C-S-H particles, leading to an increase of the packing  
392 factor of the 3 phases, analog to granular matter flow [30], better alignment  
393 of C-S-H sheets, analog to house-of-card collapse [32], ...

394 All of these hypotheses rely on the sliding of C-S-H nanoparticles, or of  
395 C-S-H sheets, enabling reorganization [33]. An alternative proposal, beside  
396 sliding, has also been made to explain the relative motion of C-S-H particles.  
397 The possibility of the existence of the dissolution-diffusion-recrystallisation  
398 series, leading to a transfer of matter among the C-S-H particles, inducing  
399 plastic strain, has also been proposed [3]. Theoretical predictions of hydrat-  
400 ing concrete creep have even been proposed [34, 35]. But these analytic laws  
401 are phenomenological and postulate a priori the existence of a significant in-  
402 fluence of the applied stress on the dissolution of the hardened material. We  
403 have shown here that this influence is significant and measurable in the case  
404 of wet gypsum and want to discuss here the case of hydrated cement.

405 Hydrated cement pastes share common characteristics with gypsum plas-  
406 ter: They both simultaneously shrink and harden during drying, they swell

407 when immersed in water after setting, and they experience humid creep. The  
 408 question of the existence of pressure solution in saturated hardened cement  
 409 arises. As for gypsum, a direct observation is not possible for the moment  
 410 and correlations have to be sought. Recent C-S-H nanoindentation measure-  
 411 ments have shown a logarithmic creep [30]. As no comprehensive model of  
 412 pressure solution creep exists, it is unfortunately not possible to draw any  
 413 conclusion about pressure solution from this logarithmic evolution of the  
 414 strain [11]. The order of magnitude of the creep compliance rate in these ex-  
 415 periments evolves from  $10^{-9}$  to  $10^{-10}$  % s<sup>-1</sup> MPa<sup>-1</sup>, for **samples ages similar**  
 416 **to ours ( $\sim 10$  days)**. In our experiments with gypsum plaster, its values is  
 417 about  $10^{-6}$  % s<sup>-1</sup> MPa<sup>-1</sup> (figure 8).

418 The crystallites in C-S-H are nanometric. The inter-particle contact  
 419 length is therefore of the same order of magnitude or lower, so 3 orders  
 420 of magnitude smaller than in set plaster, where it is micrometric (figure 4).  
 421 Therefore if pressure solution plays a role, the mass transport time between  
 422 particles should be negligible and the phenomenon should be reaction-driven,  
 423 as in the case of gypsum, and depend on the dissolution rate constant of the  
 424 material via equation 2.

425 Making the first order assumption that the correlation in gypsum plaster  
 426 and hydrated cement pastes are similar, we should have  $(\dot{\epsilon}/\sigma)_{\text{C-S-H}}/(\dot{\epsilon}/\sigma)_{\text{gypsum}} \sim$   
 427  $(ks/d)_{\text{C-S-H}}/(ks/d)_{\text{gypsum}}$ . Let us review the parameters in this equation.  
 428 The solubilities of the hydrated phases of cement depend highly on the na-  
 429 ture and structure of the phase and on the chemical environment. But the  
 430 order of magnitude of the solubility of calcium has been measured as 10  
 431 mmol/L, comparable to the 15 mmol/L solubility of calcium in the case of

432 gypsum [36]. The creep compliance rate  $\dot{\epsilon}/\sigma$  of hardened cement mentioned  
433 above are 3 orders of magnitude lower than the one of gypsum plaster. The  
434 characteristic size  $d$  of the interface between C-S-H particles is also 3 orders  
435 of magnitude lower than in gypsum plaster.

436 Therefore, a dissolution rate constant of  $k_{\text{C-S-H}} \sim 10^{-6} k_{\text{gypsum}} \sim 10^{-11}$   
437  $\text{mol m}^{-2} \text{s}^{-1}$  would enable to explain the change in the nanoparticle struc-  
438 ture responsible for the creep observed in the experiments of Vandamme &  
439 Ulm [30]. Measurements with radiotracers of the dissolution rate of C-S-H  
440 suspensions in aqueous solutions have brought a value  $k_{\text{C-S-H}} \sim 3 \times 10^{-12}$   
441  $\text{mol m}^{-2} \text{s}^{-1}$  [37]. This value is of the same order of magnitude as the value  
442 we think necessary to make pressure solution active during C-S-H creep.  
443 Therefore this order of magnitude analysis brings pressure solution among  
444 the possible phenomena acting in the creep of C-S-H.

445 We would like to stress on the fact that our assumption is consistent with  
446 all the creep models mentioned above. The novelty does not lie in the ge-  
447 ometry of the motion of the nanoparticles, but in the way of this motion,  
448 dissolution-recrystallisation instead of sliding. To strengthen this hypothe-  
449 sis, the measurement of the dissolution rate constant of C-S-H, and other  
450 hydrated phases, in aqueous solutions representative of the liquid present  
451 in the nanopores of hardened cement are highly desirable, essential to base  
452 on experimental evidence the contribution of pressure solution to concrete  
453 creep. Besides, if the role of dissolution is corroborated, its exact role on the  
454 creep strain will have to be specified. For instance, whether the dissolution-  
455 diffusion-precipitation sequence results in a creep strain accomodating the  
456 stress like in gypsum plaster [3], or the dissolution induces a thinning of the

457 crystallites inducing a viscoelastic strain progressively increasing with time  
458 [35], will have to be clarified.

## 459 **7. Conclusion**

460 We have performed wet bending creep tests to measure the strain rate of  
461 set plaster manufactured with various anti-creep admixtures (boric/tartaric  
462 acid, Trilon, Sequion, Dequest, STMP). Besides we have carried out holo-  
463 graphic interferometry experiments to measure the dissolution rate constant  
464 of gypsum in water containing these anti-creep admixtures, and the diffusion  
465 coefficient of dissolved gypsum in these solutions. A strong correlation has  
466 been found between the wet creep strain rate and the dissolution rate con-  
467 stant of the material. This clear dissolution-creep link has enabled to propose  
468 reaction-driven pressure solution creep as the underlying mechanism of the  
469 wet creep of gypsum plaster. This is the first time that this phenomenon is  
470 evidenced **experimentally in an industrial material**.

471 Following the study of gypsum plaster, an order of magnitude analysis  
472 has shown that pressure solution may also contribute to the creep of hydrated  
473 Portland cement. Indeed, alternatively to the sliding between the hydrated  
474 phase nanoparticles, the dissolution-diffusion-recrystallization sequence was  
475 shown to be another mean of the reorganization of the nanoparticles during  
476 creep.

## 477 **Acknowledgements**

478 We thank Elisabeth Charlaix, Ellis Gartner, François Renard et Dag Dys-  
479 the for fruitful discussions. This work was supported by Lafarge Centre de

480 Recherche, Région Rhône-Alpes and CNES (french spatial agency).

## 481 **References**

- 482 [1] E. Pachon-Rodriguez, E. Guillon, G. Houvenaghel, J. Colombani, Pres-  
483 sure solution as origin of the humid creep of a mineral material, *Phys.*  
484 *Rev. E* 84 (2011) 066121.
- 485 [2] Z. Chen, S. Sucech, K. Faber, A hierarchical study of the mechanical  
486 properties of gypsum, *J. Mater. Sci.* 45 (2010) 4444.
- 487 [3] J. Chappuis, A model for a better understanding of the cohesion of  
488 hardened hydraulic materials, *Colloids Surf. A* 156 (1999) 223.
- 489 [4] E. M. Gartner, Cohesion and expansion in polycrystalline solids formed  
490 by hydration reactions - the case of gypsum plasters, *Cem. Concr. Res.*  
491 39 (2009) 289.
- 492 [5] M. Sâadaoui, S. Meille, P. Reynaud, G. Fantozzi, Internal friction study  
493 of water effect on set plaster, *J. Eur. Ceram. Soc.* 25 (2005) 3281.
- 494 [6] E. Badens, S. Veessler, R. Boistelle, D. Chatain, Relation between  
495 young's modulus of set plaster and complete wetting of grain bound-  
496 aries by water, *Colloids Surf. A* 156 (1999) 373.
- 497 [7] P. Coquard, R. Boistelle, Water and solvent effects on the strength of  
498 plaster, *Int. J. Rock Mech. Min. Sci. & Geomech. Abstr.* 31 (1994) 517.
- 499 [8] H. Andrews, The effect of water contents on the strength of calcium  
500 sulfate plaster products, *J Soc. Chem. Ind.* 5 (1946) 125.

- 501 [9] H. Sattler, Elastic and plastic deformations of plaster units under uni-  
502 axial compressive stress, *Mater. Struct.* 7 (1974) 159.
- 503 [10] W. Craker, K. Schiller, Plastic deformation of gypsum, *Nature* 193  
504 (1962) 672.
- 505 [11] J. Gratier, D. Dysthe, F. Renard, The role of pressure solution creep in  
506 the ductility of the earths upper crust, *Adv. Geophys.* 54 (2013) 47.
- 507 [12] S. deMeer, C. Spiers, Creep of wet gypsum aggregates under hydrostatic  
508 loading conditions, *Tectonophys.* 245 (1995) 171.
- 509 [13] S. deMeer, C. Spiers, Uniaxial compaction creep of wet gypsum aggre-  
510 gates, *J. Geophys. Res.* 102 (1997) 875.
- 511 [14] M. Murat, L. Pusztaszeri, M. Gremion, Corrélation texture cristalline-  
512 propriétés mécaniques de plâtres durcis. étude préliminaire, *Mater.*  
513 *Struct.* 8 (1974) 377.
- 514 [15] A. Lewry, J. Williamson, The setting of gypsum plaster Part II The  
515 development of microstructure and strength, *J. Mater. Sci.* 29 (1994)  
516 5524.
- 517 [16] F. Renard, D. Dysthe, J. Feder, K. Bjorlykke, B. Jamtveit, Enhanced  
518 pressure solution creep rates induced by clay particles: Experimental  
519 evidence in salt aggregates, *Geophys. Res. Lett.* 28 (2001) 1295–1298.
- 520 [17] R. Raj, Creep in polycrystalline aggregates by matter transport through  
521 a liquid phase, *J. Geophys. Res.* 87 (1982) 4731.

- 522 [18] S. Meille, M. Sâadaoui, P. Reynaud, G. Fantozzi, Mechanisms of crack  
523 propagation in dry plaster, *J. Eur. Ceram. Soc.* 23 (2003) 3105.
- 524 [19] A. Lasaga, A. Luttge, A model for crystal dissolution, *Eur. J. Mineral.*  
525 15 (2003) 603.
- 526 [20] J. Colombani, Measurement of the pure dissolution rate constant of a  
527 mineral in water, *Geochim. Cosmochim. Acta* 72 (2008) 5634.
- 528 [21] J. Colombani, Dissolution measurement free from mass transport, *Pure*  
529 *Appl. Chem.* 85 (2013) 61.
- 530 [22] J. Colombani, J. Bert, Holographic interferometry study of the dissolu-  
531 tion and diffusion of gypsum in water, *Geochim. Cosmochim. Acta* 71  
532 (2007) 1913.
- 533 [23] E. Pachon-Rodriguez, J. Colombani, Pure dissolution kinetics of an-  
534 hydrite and gypsum in inhibiting aqueous salt solutions, *AIChE J.* 59  
535 (2013) 1622.
- 536 [24] D. Dysthe, Y. Podladchikov, F. Renard, J. Feder, B. Jamtveit, Universal  
537 scaling in transient creep, *Phys. Rev. Lett.* 89 (2002) 246102.
- 538 [25] D. Hoxha, F. Homand, C. Auvray, Deformation of natural gypsum rock:  
539 Mechanisms and questions, *Eng. Geol.* 86 (2006) 1.
- 540 [26] A. Allen, J. Thomas, H. Jennings, Composition and density of nanoscale  
541 calcium-silicate-hydrate in cement, *Nature materials* 6 (2007) 311.

- 542 [27] R. J. M. Pellenq, A. Kushima, R. Shahsavari, K. J. Van Vliet, M. J.  
543 Buehler, S. Yip, F.-J. Ulm, A realistic molecular model of cement hy-  
544 drates, *Proc. Nat. Acad. Sci. USA* 106 (2009) 16102.
- 545 [28] A. Gmira, M. Zabat, R. Pellenq, H. V. Damme, Microscopic physical  
546 basis of the poromechanical behavior of cement-based materials, *Mater.*  
547 *Struct.* 37 (2004) 3.
- 548 [29] H. Jennings, Colloid model of C-S-H and implications to the problem  
549 of creep and shrinkage, *Mater. Struct.* 37 (2004) 59.
- 550 [30] M. Vandamme, F. Ulm, Nanogranular origin of concrete creep, *Proc.*  
551 *Nat. Acad. Sci. USA* 106 (2009) 10552.
- 552 [31] Z. Bazant, Prediction of concrete creep and shrinkage: past, present  
553 and future, *Nuclear Eng. Design* 203 (2001) 27.
- 554 [32] P. Acker, Swelling, shrinkage and creep: a mechanical approach to  
555 cement hydration, *Mater. Struct.* 37 (2004) 237.
- 556 [33] J. Sanahuja, L. Dormieux, Creep of a C-S-H gel: a micromechanical  
557 approach, *Int. J. Multiscale Comput. Eng.* 357 (8) 2010.
- 558 [34] Z. Grasley, D. Lange, Constitutive modeling of the aging viscoelastic  
559 properties of portland cement paste, *Mech. Time-Depend. Mater.* 11  
560 (2007) 175.
- 561 [35] M. Suter, G. Benipal, Constitutive model for aging thermoviscoelasticity  
562 of reacting concrete ii: results and discussion, *Mech. Time-Depend.*  
563 *Mater.* 14 (2010) 291.



- 564 [36] J. Chen, J. Thomas, H. Taylor, H. Jennings, Solubility and structure of  
565 calcium silicate hydrate, *Cem. Concr. Res.* 34 (2004) 1499.
- 566 [37] I. Baur, P. Keller, D. Mavrocordatos, B. Wehrli, C. Johnson,  
567 Dissolution-precipitation behaviour of ettringite, monosulfate, and cal-  
568 cium silicate hydrate, *Cem. Concr. Res.* 34 (2004) 341.